



## Article

# Innovative Sericin-Based Film-Forming Gel for Wound Healing: Development and Performance Evaluation

Suprawee Wongtechanon <sup>1,2</sup>, Chayanee Noosak <sup>1,3</sup>, Pavarish Jantorn <sup>1</sup>, Papitchaya Watcharanurak <sup>1</sup>, Piyawut Swangphon <sup>1</sup>, Warapond Wanna <sup>2</sup>  and Dennapa Saeloh Sotthibandhu <sup>1,\*</sup> 

<sup>1</sup> Faculty of Medical Technology, Prince of Songkla University, Songkhla 90110, Thailand; fongsuprawee@gmail.com (S.W.); chayanee.no@wu.ac.th (C.N.); pavarish.j@psu.ac.th (P.J.); papitchaya.w@psu.ac.th (P.W.); piyawut.s@psu.ac.th (P.S.)

<sup>2</sup> Division of Biological Science, Faculty of Science, Prince of Songkla University, Songkhla 90110, Thailand; waraporn.wa@psu.ac.th

<sup>3</sup> Department of Medical Technology, School of Allied Health Sciences, Walailak University, Nakhon Si Thammarat 80160, Thailand

\* Correspondence: dennapa.sa@psu.ac.th; Tel.: +66-7428-9133

**Abstract:** The development of effective wound dressings remains a critical challenge in medical treatments, requiring materials that promote healing, minimize infection, and enhance tissue regeneration. This study evaluated the wound-healing potential of sericin-based film-forming gels. Six formulations were developed by combining varying concentrations of sericin, a protein derived from silk cocoons, with polyvinyl alcohol (PVA). These formulations were evaluated for physical properties including drying time, pH, spreadability, stability, swelling ratio, flexibility, and adhesion. Film-forming gel is an attractive option for wound dressing due to its flexibility, adhesion, and infrequent reapplication. The F4 formulation (1% sericin) demonstrated superior performances in drying time, spreadability, stability, swelling ratio, flexibility, and skin adhesion, was easy to apply, and formed a stable film on drying. Biological evaluations showed that F4 exhibited excellent compatibility with skin fibroblast cells, maintained a suitable pH, and significantly promoted cell proliferation and migration. The F4 formulation also demonstrated anti-inflammatory effects by inhibiting iNOS expression and nitric oxide production, offering mechanical stability, biological activity, and ease of use with significant potential for treating acute and chronic wounds.

**Keywords:** film-forming gel; polyvinyl alcohol; sericin; wound healing



Academic Editor: Jana Ghitman

Received: 11 March 2025

Revised: 17 April 2025

Accepted: 20 April 2025

Published: 3 May 2025

**Citation:** Wongtechanon, S.; Noosak, C.; Jantorn, P.; Watcharanurak, P.; Swangphon, P.; Wanna, W.; Sotthibandhu, D.S. Innovative Sericin-Based Film-Forming Gel for Wound Healing: Development and Performance Evaluation. *Polymers* **2025**, *17*, 1246. <https://doi.org/10.3390/polym17091246>

**Copyright:** © 2025 by the authors. Licensee MDPI, Basel, Switzerland. This article is an open access article distributed under the terms and conditions of the Creative Commons Attribution (CC BY) license (<https://creativecommons.org/licenses/by/4.0/>).

## 1. Introduction

Wounds are physical injuries that result in the breaking of cells and membranes [1]. The disruption of structure and function in healthy skin creates a cavity that requires repair. The economic and social burden of wounds is significant. Medicare costs associated with acute and chronic wounds were estimated at \$28.1–\$96.8 billion in 2018 [2]. In the United States, medical expenses for surgical scars and injuries were around \$12 billion, while burn wounds amounted to \$7.5 billion each year [3]. The World Health Organization reported that over 300,000 people die from skin injuries annually [4]. Wound healing is a biological progression that involves four phases: homeostasis, inflammation, proliferation, and remodeling [5]. Skin tissue possesses the ability to self-repair, but certain wound types, including diabetic ulcers, burn injuries, and large surface areas or deep wounds, exhibit impaired healing processes [6]. A multifunctional wound dressing is crucial for

supporting the wound-healing process. The ideal wound dressing should be non-allergenic and minimize side effects with the ability to absorb excess wound exudate, maintain skin moisture, and stimulate wound-healing mechanisms [5].

Natural extracts have recently attracted interest in tissue engineering because of their biodegradability, biocompatibility, and bioresorbability [7]. Several natural products have shown potential as effective bioactive materials for wound healing and anti-inflammatory applications, such as gotu kola, young coconut, and silk cocoons [8–10]. Sericin extracted from silk cocoons has been studied for use in cosmetics and tissue engineering due to its excellent biological activities, biocompatibility, and low immunogenicity [11]. Sericin is usually discarded as waste from the textile industry, causing environmental contamination [4]. Previous studies indicated that sericin has remarkable properties as a wound dressing biomaterial, including anti-inflammatory effects, the promotion of cell proliferation, and the enhancement of collagen synthesis through activation of fibroblasts [12,13]. Sericin demonstrated cytoprotective and mitogenic effects on fibroblasts and keratinocytes, highlighting its potential as an option for the formulation of advanced skin and tissue regenerative materials [4]. However, sericin has poor mechanical strength, which could be improved by the combination with other biomaterials. Sericin contains hydroxyl, carbonyl, and amino groups in its side chains, allowing easy cross-linking, blending, and copolymerization with various materials [4,14]. Polyvinyl alcohol (PVA) is a synthetic polymer known for its biocompatibility, biodegradability, and affordability. PVA has outstanding mechanical and gas barrier properties, chemical resistance, and good film-forming ability [15,16]. Thus, the combination of sericin and PVA could improve the mechanical performance of sericin-based biomaterials used in wound dressing.

Various forms of sericin/PVA biomaterials have been developed for innovative wound-dressing applications, such as hydrogels, nanofibers, and films [6,15,17]. Sericin films exhibited a slow degradation rate, with increased cell adhesion and viability of the fibroblasts [10]. However, the film form has low stability, which impacts applications, depending on the specific types of wounds or individual patients. A liquid film-forming gel that transformed into a stable solid film covering the skin on drying would prolong the effectiveness of the active ingredients. A film-forming gel is also easy to apply and provides good flexibility and adhesion to the skin surface with infrequent reapplication [18].

This study developed sericin/PVA-based film-forming gels for wound-healing applications. The physical performance of formulations with various ratios of sericin were characterized and evaluated for wound dressing, including drying times, pH, spreadability, stability, and swelling ratio. The biological effects of the films were assessed by investigating their cytocompatibility with fibroblast cells, wound-healing activities, and anti-inflammatory properties.

## 2. Materials and Methods

### 2.1. Preparation of Sericin Extract

Sericin was extracted following the method used in a previous study [19]. In brief, 32 g of dry silkworm cocoons were boiled in 1 L of distilled water at 100 °C for 90 min. The sericin solution was freeze-dried using a Coolsafe Touch freeze dryer (Labogene, Bjarkesvej, Denmark).

### 2.2. Preparation of Film-Forming Gel Formulations

Polyvinyl alcohol (10% *w/v*) (PVA; Loba, Maharashtra, India) was dissolved in distilled water at 95 °C. Subsequently, 0.25%, 0.5%, and 1% (*w/v*) of sericin solution were added to the PVA solution and stirred continuously. Glycerol and 95% ethanol were immediately

added to the sericin/PVA solution and mixed homogeneously. The concentrations of components in each sericin-based film-forming gel formulation are shown in Table 1.

**Table 1.** Contents of sericin-based film-forming gel.

Formulations	Component Concentrations (%w/v)					
	10% PVA	0.25% Sericin	0.5% Sericin	1% Sericin	95% Ethanol	Glycerol
F1	6.5	-	-	0.2	7.9	6.3
F2	6.5	-	0.1	-	7.9	6.3
F3	6.5	0.05	-	-	7.9	6.3
F4	6.5	-	-	0.15	11.85	6.3
F5	6.5	-	0.075	-	11.85	6.3
F6	6.5	0.0375	-	-	11.85	6.3

### 2.3. Determination of Film Evaporation Times on the Skin and the Slide

The drying times of the films were determined on the skin and the slide. One hundred microliters of each formulation were applied to either the skin of a stillborn piglet or a glass slide, each with an area of  $2.5 \times 2.5 \text{ cm}^2$ . Drying times were recorded by gently touching the skin or glass slide, and the integrity of the dried film on the skin was subsequently assessed [20].

### 2.4. Determination of pH

The pH values of all the formulations were measured in triplicate with a Eutech™ pH 700 meter (Thermo Scientific, Waltham, MA, USA).

### 2.5. Determination of Spreadability

One gram of each formulation was dropped onto a glass plate and covered with another glass plate. The time taken to spread was recorded, with the spreadability calculated using the following equation:

$$\text{Spreadability} = \frac{W \times A}{T} \quad (1)$$

where W is the weight of the formulation, A is the area of the glass plate, and T is the spread time.

### 2.6. Assessment of Stability

All formulations were kept at 4 and 25 °C for 30 and 60 days. The evaporation time on the skin and the glass slide, pH, and spreadability were recorded and analyzed.

### 2.7. Evaluation of Swelling Ratio

A 50 µL aliquot of all the formulations was dropped onto a glass slide with an area of  $1 \times 1 \text{ cm}$ . The formulations were dried in an incubator at 60 °C overnight. The films were then weighed. The dry weight was recorded before the films were immersed in phosphate-buffered saline (PBS) and incubated at 37 °C. The films were weighed at 1, 2, 4, 8, and 12 h. The swelling ratio was calculated using the following equation:

$$\text{Swelling ratio}(\%) = \left( \frac{W_s - W_d}{W_d} \right) \quad (2)$$

where  $W_s$  is the weight of the swelled sample and  $W_d$  is the weight of the dry sample.

### 2.8. Collection of Film-Forming Gel Supernatant

The F4, F5, and F6 formulations were dried in a 24-well plate. Dulbecco's Modified Eagle Medium (DMEM; Gibco, Grand Island, NY, USA) containing 10% fetal bovine serum (FBS; Gibco, Grand Island, NY, USA) and 1% antibiotic–antimycotic (Gibco, Grand Island, NY, USA) was added to the film surface and incubated under 5% CO<sub>2</sub> at 37 °C. At specific times, the film supernatant was collected for the following experiments.

The supernatants of the film-forming gel collected at 3, 6, 12, 18, and 24 h were measured at a wavelength of 420 nm to determine the sericin release.

### 2.9. Fibroblast Cell and Macrophage Cell Culture

Fibroblast L929 cells and macrophage RAW 264.7 cells were cultured in DMEM medium containing 10% FBS and 1% antibiotic–antimycotic under 5% CO<sub>2</sub> at 37 °C. After reaching confluence, the cells were harvested using Trypsin-EDTA (Gibco, USA).

### 2.10. Evaluation of Cell Viability

The cell viability was determined by the MTT assay. Fibroblast L929 cells were seeded at a density of  $2 \times 10^4$  cells/well into a 96-well plate and incubated overnight under the condition previously described. The cells were treated with the film-forming gel supernatants collected at 6, 12, and 24 h. After 24 h of incubation, the cell viability was analyzed using MTT reagent (Alfa Aesar, Heysham, Lancashire, UK), and the absorbance was measured at a wavelength of 570 nm. The total cell viability was calculated by the following equation:

$$\text{Cell viability(\%)} = \frac{AT}{AC} \times 100 \quad (3)$$

where AT is the absorbance of treated cells, and AC is the absorbance of untreated cells.

### 2.11. Scratch Wound Assay

Fibroblast L929 cells were seeded at a density of  $1 \times 10^5$  cells/well in 24-well plates and cultured for 24 h under 5% CO<sub>2</sub> at 37 °C. The cell monolayer was scratched with a sterile tip across the center of each well. The cells were washed with the culture medium to remove the detached cells and subsequently treated with the film-forming gel supernatant collected at 24 h. The cells with the culture medium were used as a control. Wound-healing efficiency was monitored at 0, 12, and 24 h. The scratch closure rate was calculated using the following equation:

$$\text{Scratch closure rate} = \frac{A_{t0} - A_t}{A_{t0}} \times 100 \quad (4)$$

where  $A_{t0}$  is the scratch area at time 0 h, and  $A_t$  is the comparable scratch area at 12 and 24 h.

### 2.12. Determination of Nitric Oxide Concentration

Nitric oxide (NO) production was determined according to the nitrite levels by the modified Griess assay. The macrophage RAW 264.7 cells were cultured on high glucose-DMEM (Sigma Aldrich, St. Louis, MO, USA) supplemented with 10% FBS and 1% antibiotic–antimycotic at 37 °C under 5% CO<sub>2</sub>. The cells were seeded at a density of  $5 \times 10^4$  cells/well into a 96-well plate. After incubation, the cells were pre-treated with the film supernatant collected at 6, 12, and 24 h for 4 h. Lipopolysaccharide (LPS) at 1 µg/mL was added to each well and further incubated for 24 h. Subsequently, the culture medium from each well was collected and incubated with a modified Griess reagent (Sigma-Aldrich, USA) for 15 min in the dark. The absorbance was measured at a wavelength of 540 nm to calculate the NO concentration.

### 2.13. Real-Time Quantitative PCR Analysis

The macrophage RAW 264.7 cells were seeded in a 96-well plate at a density of  $5 \times 10^4$ /well and cultured for 24 h under 5% CO<sub>2</sub> at 37 °C. The cells were pre-treated with the F4 supernatant collected at 12 h for 4 h. Then, LPS was added to each well and further incubated for 24 h. Cells treated with dexamethasone (10 µM) containing LPS (1 µg/mL) were used as a control. The total RNA concentration was extracted using a total RNA mini kit (Geneaid Biotech Ltd., New Taipei City, Taiwan), and the purified RNA samples were detected by a Nanodrop spectrophotometer (Thermo Scientific, USA). The total RNA of each sample was used for reverse transcription into cDNA using a RevertAid First Strand cDNA synthesis kit (Thermo Scientific, USA). Quantitative reverse transcription PCR (RT-qPCR) was determined using a Bio-Rad real-time PCR CFX96 (Bio-Rad, Hercules, CA, USA). The RT-qPCR analysis was performed using an EvaGreen PCR reagent kit (Solis Biodyne, Tartu, Estonia). The relative amount of gene expression was determined using the  $2^{-\Delta\Delta C_q}$  method. The specific primers used in this study are shown in Table 2.

**Table 2.** Primers used in this study.

Primer	Sequence (5'-3')	Reference
<i>iNOS</i>	Forward: CACCACCCTCCTTGTTCAAC Reverse: CAATCCACAACCTCGCTCCAA	[21]
<i>GAPDH</i>	Forward: CATGGCCTTCCGTGTTCTTA Reverse: CCTGCTTCACCACCTTCTTGAT	

### 2.14. Western Blot Assay

The RAW 264.7 cells were seeded in 6-well plates at a density of  $5 \times 10^5$  cells/well. The cells were pre-treated with the F4 supernatant collected at 12 h for 4 h and stimulated with LPS (1 µg/mL) for 24 h. The total protein in the cells was extracted using a radioimmunoprecipitation assay buffer (RIPA; Servicebio, Wuhan, Hubei, China), with protein concentrations determined using a Pierce BCA protein assay kit (Thermo Scientific, Rockford, IL, USA). Equal quantities (20 µg) of protein samples were separated by SDS-PAGE and transferred into a polyvinylidene difluoride (PVDF) membrane (Servicebio, Wuhan, Hubei, China). The membranes were probed with primary antibodies including anti-iNOS and anti-β-actin (Cell Signaling, Danvers, MA, USA) overnight, and the horseradish peroxidase-linked secondary antibody (Cell Signaling, Danvers, MA, USA) for 1 h at room temperature. β-actin was used as an internal control. Protein bands were detected by enhanced chemiluminescence (ECL) Western blotting detection reagent (Servicebio, Wuhan, Hubei, China) and visualized using ChemiDoc Imaging (Bio-Rad, Hercules, CA, USA).

### 2.15. Statistical Analysis

The values shown are the means of the three wells from three independent experiments. Statistical significance was determined using a two-way Student's *t*-test for independent means using Microsoft Excel. Data are presented as the mean ± SD of three independent experiments, with *p* < 0.05 considered statistically significant.

## 3. Results and Discussion

### 3.1. Characteristics and Physical Properties of the Film-Forming Gels

#### 3.1.1. Characteristics of the Film-Forming Gel

Sericin and PVA film-forming gels were developed for wound-healing applications. The combination of sericin with PVA was chosen due to its favorable properties for wound

healing. While other combinations of sericin with different polymers exist, PVA was selected for its unique advantages. For example, although chitosan contains  $\text{NH}_2$  groups that offer antimicrobial benefits, it tends to be less flexible and has lower film-forming ability than PVA [22]. Alginate, which contains  $\text{COOH}$  groups and is highly absorbent, does not provide the same stability or film-forming strength as PVA [23]. Gelatin, with its amino acid residues, supports cell attachment but may be less stable and degrade more easily in moist conditions [24]. In contrast, PVA, which contains hydroxyl ( $-\text{OH}$ ) groups, offers excellent film-forming ability, flexibility, and moisture retention, all of which are crucial for maintaining an optimal environment for wound healing [25]. Our previous study demonstrated that the combination of PVA and sericin significantly improved the mechanical and biological properties of hydrogels, enhancing their effectiveness in supporting tissue repair in orthopedic applications [26]. When combined with sericin, which contributes bioactive properties that promote tissue regeneration, PVA provides a balanced combination of structural integrity and biological activity, making it an ideal choice for wound-healing applications.

Sericin was incorporated as a bioactive component due to its proven biological activities, including stimulation of collagen synthesis and promotion of fibroblast migration [27]. Additionally, glycerol was added to the formulation as a plasticizer to improve the flexibility of the dried film and prevent cracking over time [28]. It also helped in moisture retention and influenced phase separation between sericin and PVA [29]. Furthermore, ethanol was included to enhance permeability and reduce the drying time of the gel, facilitating faster film formation upon application.

All dry films obtained from the film-forming gel solution exhibited transparency with a light-yellow color and formed a complete film with no cracking or flaking (Figure 1). The characteristics of the different sericin-based film-forming gel formulations are shown in Table 3. The film-forming gel formulations were applied to the skin and slide to determine the drying time. The evaporation test performed on the slide negated various skin factors that influenced drying time, such as skin humidity and individual skin characteristics, providing a more standardized and reproducible measurement of drying time.

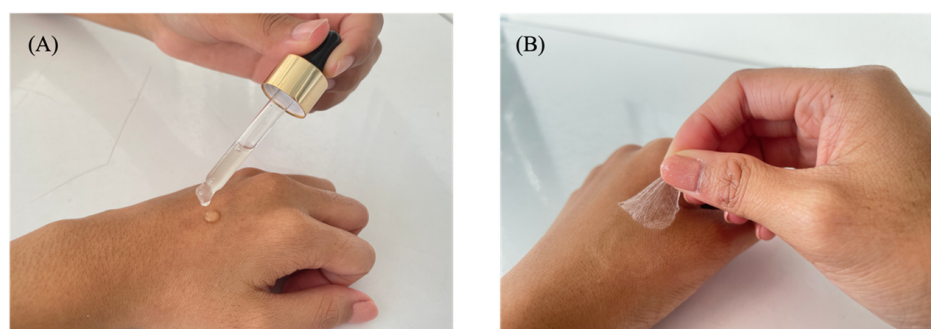


**Figure 1.** Representative images of sericin-based film-forming gel. (A) Gel stage, (B) Film stage.

**Table 3.** Characteristics of different sericin-based film-forming gel formulations.

Formulation	Integrity on Skin	Drying Time (min)		pH	Spreadability ( $\text{g cm}^2/\text{s}$ )
		On Skin	On Glass Slide		
F1	a	$4.29 \pm 0.45$	$9.06 \pm 0.22$	$5.22 \pm 0.03$	$1.48 \pm 0.13$
F2	a	$4.54 \pm 0.27$	$8.28 \pm 0.20$	$5.25 \pm 0.02$	$1.59 \pm 0.04$
F3	a	$4.43 \pm 0.30$	$9.31 \pm 0.05$	$5.23 \pm 0.01$	$1.98 \pm 0.10$
F4	a	$3.54 \pm 0.52$	$6.54 \pm 0.18$	$5.30 \pm 0.01$	$1.54 \pm 0.03$
F5	a	$4.18 \pm 0.05$	$7.05 \pm 0.15$	$5.37 \pm 0.02$	$2.39 \pm 0.06$
F6	a	$4.18 \pm 0.21$	$6.35 \pm 0.26$	$5.36 \pm 0.02$	$2.31 \pm 0.04$

Note: a = complete film with no cracking or flaking.

The formulations F4, F5, and F6 exhibited shorter drying times compared to F1, F2, and F3 on the skin (3–4 min vs. 4–5 min) and on the slide (6–7 min vs. 8–10 min), Table 3. This difference was attributed to the higher ethanol content in the F4, F5, and F6 formulations, which accelerated the evaporation process. Similar trends were observed in other studies. For example, in an etoricoxib film-forming gel study, drying times ranged from 3–6 min, with 10 out of 17 formulations drying at similar rates and comparable to our F1–F6 formulations [30]. In a terbinafine hydrochloride-loaded film-forming gel study, the first two formulations dried faster (2–3 min), while the remaining formulations had similar drying times [31]. These results mirrored our findings, where formulations with higher ethanol content (F4, F5, F6) dried faster than those with lower ethanol content (F1, F2, F3), suggesting that the ethanol content played a significant role in reducing drying times across different formulations and supporting the idea that a higher ethanol volume promoted faster evaporation [32]. By contrast, a study on a film-forming polymeric dispersion containing *Centella asiatica* reported a longer drying time of 10–15 min to form a film [33], slower than the drying times observed in our study. This result highlighted how different formulation compositions can significantly influence the drying behavior of film-forming gels.

The pH of the formulations played an important role in their skin compatibility. Topical formulations should be acidified to achieve a pH level ranging between 4.1 and 5.8 [34]. As shown in Table 3, the pH values of the F1, F2, and F3 formulations were lower than those of the F4, F5, and F6 formulations, which ranged from 5.2 to 5.4. The pH of sericin was recorded as  $5.97 \pm 0.04$ , with PVA  $5.12 \pm 0.03$ . The pH values of glycerol and ethanol were  $3.35 \pm 0.02$  and  $6.76 \pm 0.02$ , respectively. The F4, F5, and F6 formulations, which contained high volumes of ethanol, demonstrated increased pH values. A previous study recorded the natural pH of the skin of 330 human volunteers as 4.0 to 7.0 [35]. Therefore, the obtained skin pH could be applied in the development of effective topical products. All the formulations revealed suitable pH values, suggesting compatibility with the skin while minimizing the risk of irritation.

Spreadability is a characteristic used to assess the spread of film-forming gel on the skin surface. A consistent standard dose of a medicated formulation must be delivered to the skin to ensure the efficacy of a topical treatment. The spreadability values of the F1 and F4 formulations were lower than those of the other four formulations because the sericin extract became a gel and formed a film [36]. Generally, films with low spreadability tend to be more effective because they are easy to apply and enhance adherence to the skin during use [37]. Films with low spreadability reduce the risk of unintended movement from the applied area, which is an advantage for targeted treatments. The results demonstrated that the F1 and F4 formulations exhibited low spreadability, indicating ease of application and enhanced usability on the skin.

The stability of the formulations was compared at three time points: initial time, 30 days, and 60 days, under controlled temperature conditions of 4 °C and 25 °C. All the formulations presented homogeneous gels. The dry films obtained from the film-forming gel solutions were light transparent yellow, with no cracking or flaking in the complete film. Figure 2 shows the properties of film-forming gels under various conditions. The drying time of the film on the skin ranged from 3.5–5 min, whereas the drying time on the glass slide was stable at 7–9 min, exhibiting longer drying time on the skin and the slide compared to the initial time (Figure 2A,B). The spreadability of the formulations remained consistent with the initial time at all temperatures after 30 days and 60 days of storage (Figure 2C). The pH of the formulations exhibited stability over 60 days, maintaining values within the range of 5–6 (Figure 2D). Ethanol plays a crucial role in enhancing the self-preserving system, contributing to the stability and safety of the final product [38].

A previous study demonstrated that ethanol could be used as a solvent, skin enhancer, and preservative of hydroalcoholic gels for topical administration [39]. Glycerol was also reported as a plasticizer and stabilizer solution for film formation and gel structure [40,41]. In the formulation, alcohol acted as a preservative, while glycerol functioned as a plasticizer and stabilizer, contributing to the overall stability and integrity of the product. The findings indicated that 4 °C and 25 °C were the optimal storage conditions for all the formulations to prevent degradation or loss of effectiveness over time.

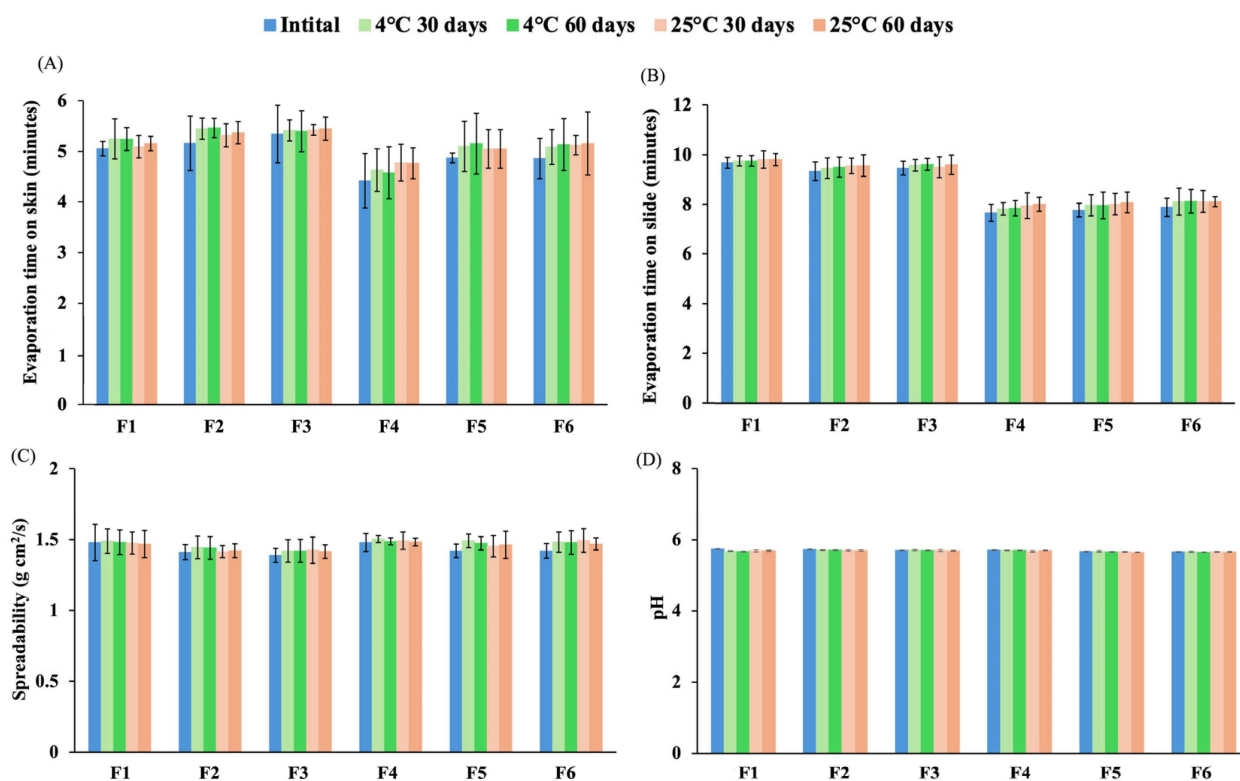


**Figure 2.** Physical stability of sericin-based film-forming gel under different conditions. (A) Evaporation time on the skin, (B) Evaporation time on the glass slide, (C) Spreadability, and (D) pH of the formulations.

### 3.1.2. Swelling Capacity of the Film-Forming Gels

Wound dressing biomaterials should effectively absorb excess exudate from the wound while maintaining a moisture-proof environment to support the healing process [5]. Our formulations contain glycerol, which acts as a moisturizer by keeping the skin moist, protecting it from excessive drying, and preventing moisture loss through the formation of a protective barrier [42]. Sericin, also present in the formulations, is rich in polar amino acids, including serine, aspartic acid, and glutamic acid. These amino acids contribute to sericin's hydrophilic nature, enhancing its ability to absorb and retain moisture [43,44].

To evaluate the water absorption capacity of each formulation, the swelling ratio was measured. As shown in Figure 3, the F1 formulation exhibited the greatest swelling ratio, followed by F2 and F3 (Figure 3A), while F4 demonstrated more swelling than F5 and F6 (Figure 3B). Formulations F1 and F4, which contained 1% sericin, showed higher swelling ratios compared to those with 0.5% and 0.25% sericin. These findings highlight the significant role of sericin in enhancing water absorption, which may contribute to the effective management of exudate in wound care. Consistent with previous studies, sericin enhanced the swelling capability of the hydrogel, showing an increase of up to 15% after immersion in PBS for 4 h [45].

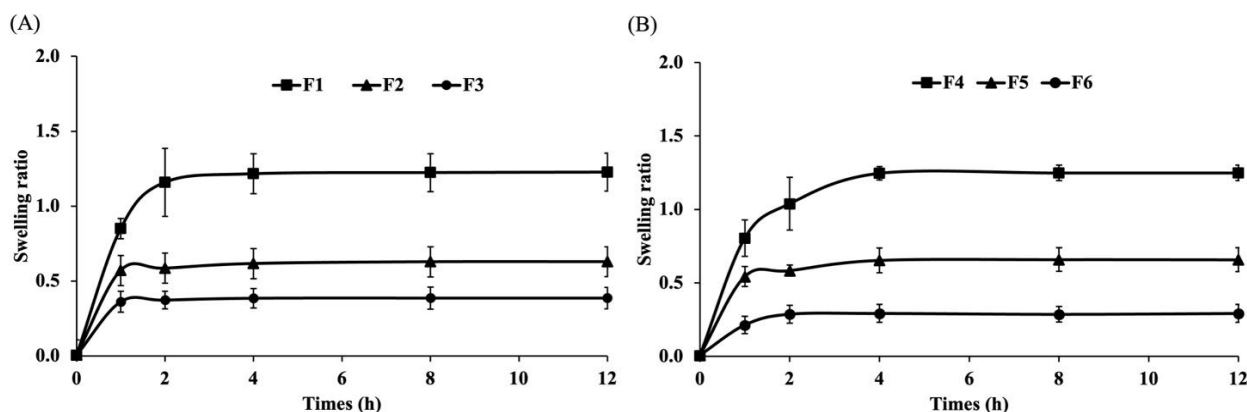


**Figure 3.** Swelling ratios of sericin-based film-forming gels at different times. (A) F1, F2, and F3 and (B) F4, F5, and F6.

### 3.2. Biological Activities of the Film-Forming Gels

#### 3.2.1. Effects on Wound Healing

Based on the gel characteristics and physical testing experiments, the F4, F5, and F6 formulations were selected for subsequent biological evaluation. The MTT assay was carried out to assess the cytotoxicity of film-forming gels on fibroblast cells. The supernatants from the F4, F5, and F6 formulations were used to treat L929 fibroblast cells, with the corresponding percentages of cell viability shown in Figure 4. The formulations revealed no cytotoxicity, with F4 significantly enhancing cell proliferation compared to the untreated cells after 12 and 24 h ( $p < 0.05$ ). Sericin enhanced fibroblast cell proliferation without inducing cytotoxic effects, potentially improving wound healing and skin regeneration applications in biomedical fields [10]. The F4 formulation containing the highest concentration of 1% sericin extract showed enhanced cell proliferation compared to F5 and F6.

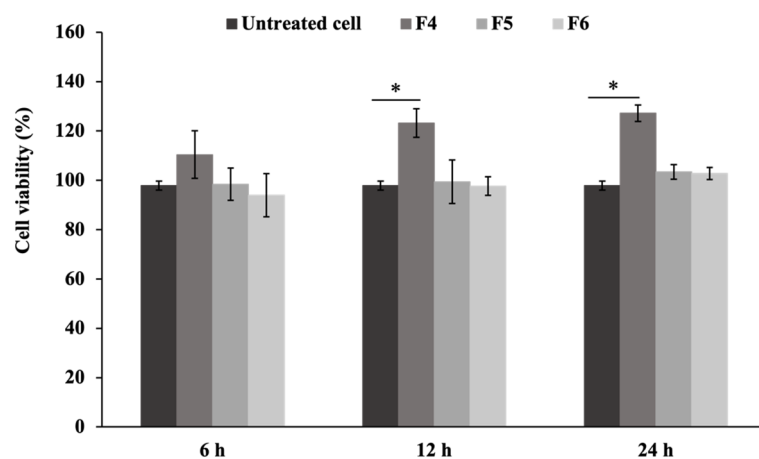


**Figure 4.** The effects of F4, F5, and F6 supernatants on the viability of the L929 cell line at 6, 12, and 24 h (\*  $p < 0.05$  compared to untreated cells).

Fibroblasts in healthy skin are essential for connective tissue regeneration and the remodeling of tissues. Sericin facilitates the synthesis of type I collagen, which plays a critical role in collagen biosynthesis and is fundamental to the wound-healing process [27]. In this study, the scratch assay was applied to evaluate the effects of film-forming gel on fibroblast cell migration. The progression of wound closure was monitored at 12 and 24 h post-scratching and expressed as the percentage of wound healing over time (Figure 5A,B). The F4 formulation exhibited the most effective in cell migration, indicating enhanced wound healing compared to untreated cells and revealed the highest percentage of wound

closure after 24 h at 89%, demonstrating a significant increase compared to F5 and F6 ( $p < 0.05$ ). Previous studies found that sericin effectively stimulated fibroblast proliferation and migration by increasing cell adhesion and promoting mitogenic effects on mammalian cells [46,47]. This enhancement positively contributed to the wound-healing process, facilitating improved tissue regeneration and repair. Sericin release (Figure 5C) from the F4 formulation was significantly higher than from the F5 and F6 formulations ( $p < 0.05$ ). A gradual release was sustained over 24 h, as one characteristic desired for wound treatment applications [48]. These findings suggested that the higher sericin content in F4 was associated with enhancing wound closure. Therefore, F4 showed promise as a biomaterial that effectively promoted wound healing.

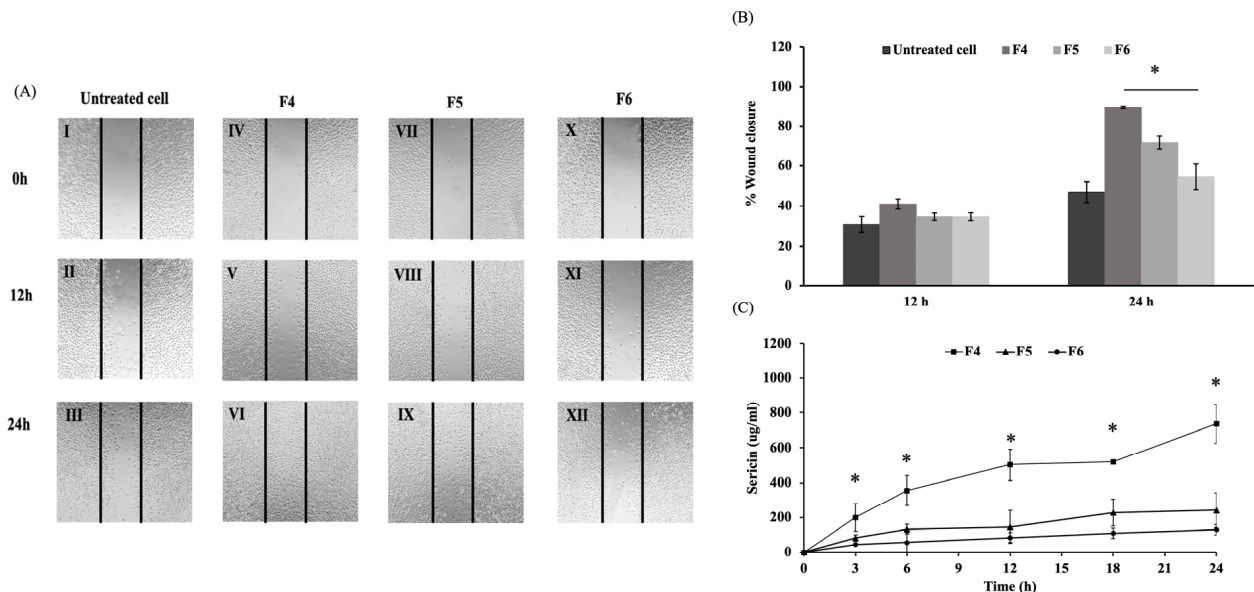


**Figure 5.** (A) Scratch assay of L929 cell line treated with F4, F5, and F6 supernatant at 12 and 24 h. I–III: Untreated cells, IV–VI: F4, VII–IX: F5, and X–XII: F6. Black lines mark the margins of the wound at 0 h in each photomicrograph. (B) Quantitative analysis of scratch closure after 12 and 24 h. (C) Sericin release from the F4, F5, and F6 formulations immersed in PBS at different times, with absorbance measured at 420 nm (\*  $p < 0.05$  compared to F4).

### 3.2.2. Effects on Inflammatory Response

Nitric oxide (NO) is a signaling molecule that plays a crucial role in regulating a wide range of cellular processes in the human body under normal physiological conditions and in pathological states. These processes include vasodilation, neurotransmission, inflammation, apoptosis, and tumorigenesis [49]. Elevated levels of nitric oxide trigger immune responses and drive the inflammatory cascade during inflammatory conditions. Activated macrophages stimulate the expression of inducible nitric oxide synthase (iNOS), which subsequently leads to the production of NO [50]. The inhibitory effects of the formulations on NO synthesis were evaluated in LPS-stimulated RAW 264.7 cells, with the F4, F5, and F6 formulations identified as promising anti-inflammatory agents. As shown in Figure 6A, NO production was almost undetectable in the unstimulated cells, whereas the LPS significantly induced NO production in RAW 264.7 cells compared to the untreated cells ( $p < 0.05$ ). Dexamethasone, a commonly used drug for the treatment of inflammatory conditions, was used as a positive control in the experiment [51]. Dexamethasone significantly reduced the NO level compared to the LPS-treated cells ( $p < 0.05$ ). The F4, F5, and F6 formulations significantly reduced NO in the LPS-induced cells at 6, 12, and 24 h compared to LPS-treated cells ( $p < 0.05$ ). F4 significantly reduced NO production compared to the F5 and F6 formulations at 12 h ( $p < 0.05$ ), while F5 demonstrated a significant decrease in

NO compared to F6 at 12 h ( $p < 0.05$ ). Therefore, the F4 formulation at 12 h, which strongly suppressed LPS-induced NO production in RAW 264.7 cells, was chosen for subsequent experiments in gene and protein expression.

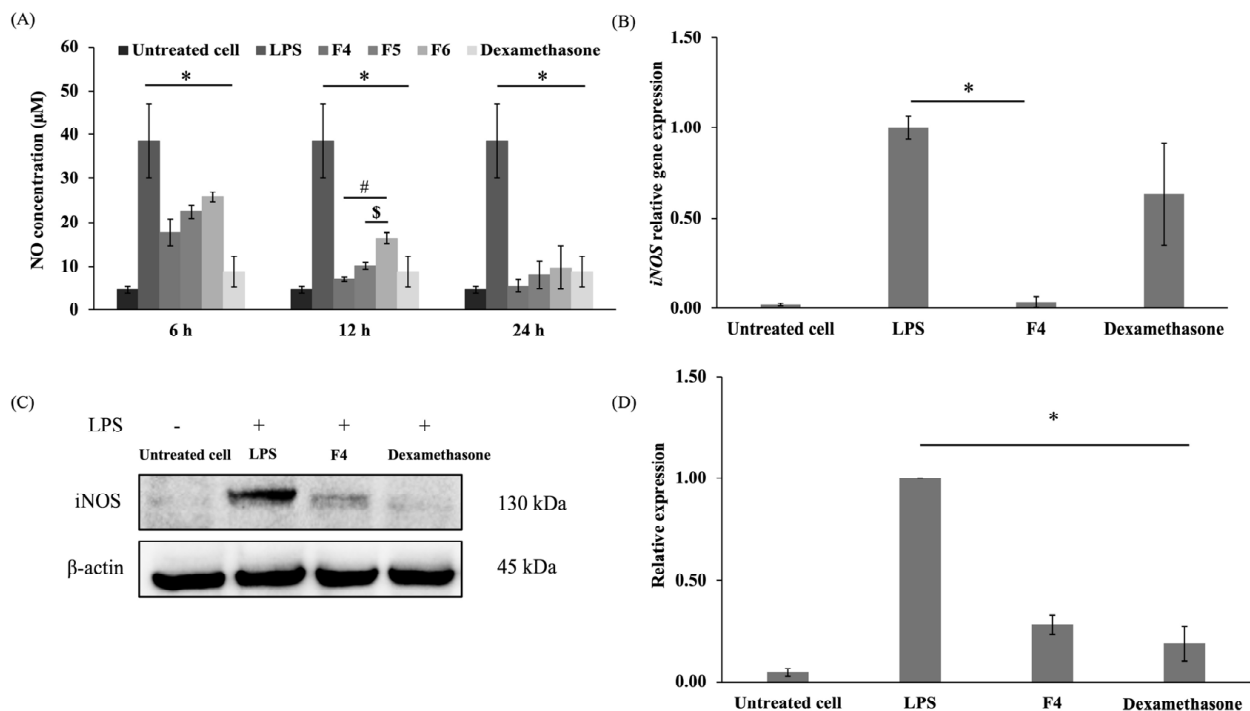


**Figure 6.** Anti-inflammatory effects of film-forming gel formulations on LPS-induced RAW 264.7 cells. (A) NO production, (B) *iNOS* gene expression normalized to *GAPDH*, (C) Expression of *iNOS* determined by Western blot analysis, (D) *iNOS* protein expression normalized to  $\beta$ -actin (\*  $p < 0.05$ ; film-forming gel formulations compared to LPS-stimulated RAW 264.7 cells, #  $p < 0.05$ ; F4 compared to F5 and F6, \$  $p < 0.05$ ; F5 compared to F6).

The mRNA expression of *iNOS* was significantly upregulated in the LPS-induced macrophage cells ( $p < 0.05$ ) (Figure 6B). A previous study found that dexamethasone reduced the mRNA expression of *iNOS* by inhibiting NF- $\kappa$ B and AP-1, transcription factors that regulate *iNOS* expression in the inflammatory process [51]. However, dexamethasone does not directly bind to *iNOS*. The F4 formulation significantly downregulated *iNOS* expression levels compared to the LPS-stimulated cells ( $p < 0.05$ ), demonstrating that sericin in the formulation possessed a potent anti-inflammation capacity.

*iNOS* is a crucial enzyme in the inflammatory process that regulates multiple key mechanisms associated with intracellular signaling in different cells or species [52,53]. In macrophages, *iNOS* generates excessive NO in response to inflammation induced by LPS [50]. As shown in Figure 6C,D, the level of *iNOS* protein was upregulated in LPS-stimulated cells. By contrast, the F4 formulation and dexamethasone significantly suppressed *iNOS* protein expression ( $p < 0.05$ ). These results confirmed the biological activity of sericin, which plays a significant role in modulating the inflammatory response by reducing the expression of *iNOS*.

Inflammation is a biological defense mechanism that may occur in response to wound infection and tissue damage, leading to the generation of new tissue to repair damage [46]. Nuclear factor kappa B (NF- $\kappa$ B) controls the duration of inflammation by regulating cytokines and *iNOS* [54]. The suppression of NF- $\kappa$ B activity decreases *iNOS* transcription and subsequently reduces the excessive production of NO in macrophages [55]. Previous studies demonstrated that sericin inhibited *iNOS* expression [13,56]. Sericin reduced the production of pro-inflammatory cytokines including TNF- $\alpha$ , IL-1 $\beta$ , and IL-6 which are

critical upstream regulators of iNOS [57]. The F4 formulation containing 1% sericin showed significant anti-inflammatory effects by suppressing the iNOS protein, thereby reducing *iNOS* gene expression and NO production (Figure 7).

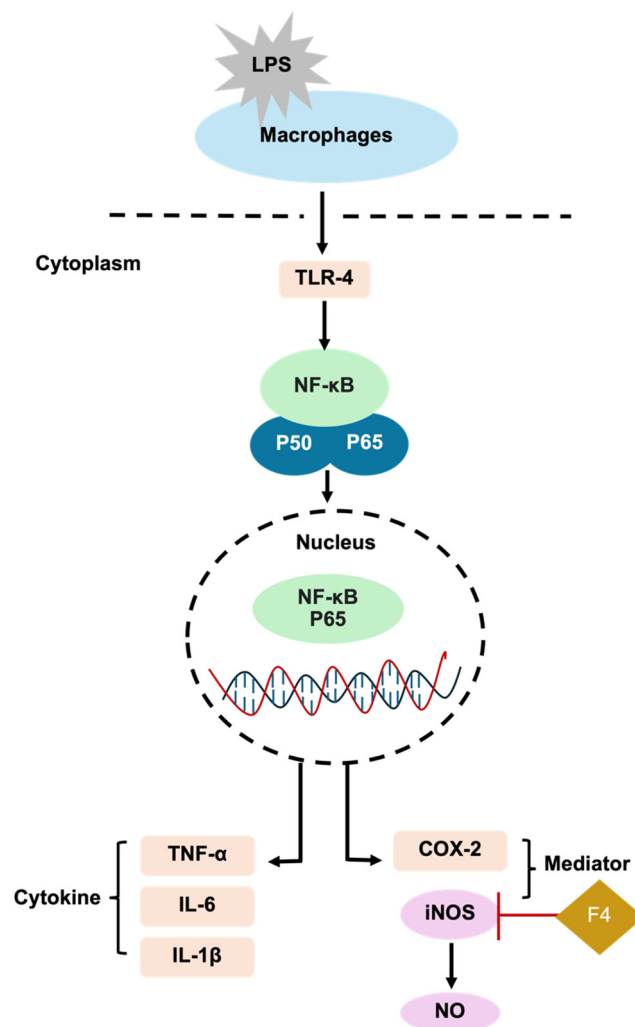


**Figure 7.** Proposed anti-inflammatory mechanism of the F4 formulation in suppressing iNOS in LPS-induced RAW 264.7 macrophage cells.

#### 4. Conclusions

This study evaluated sericin-based film-forming gel formulations for wound dressing applications, focusing on their physical and biological properties. The F4 formulation containing 1% sericin demonstrated superior drying time, spreadability, stability, and swelling ratio. The F4 formulation also exhibited excellent compatibility with skin fibroblast cells, maintaining pH levels within the acceptable range of  $3.54 \pm 0.52$ . Biological evaluations revealed that F4 significantly promoted cell proliferation and migration and exhibited anti-inflammatory effects by inhibiting iNOS expression and nitric oxide production. These findings highlighted F4 as a promising candidate for wound-healing applications, showing effective anti-inflammatory and regenerative properties.

**Author Contributions:** Conceptualization, D.S.S.; Data curation, S.W. and D.S.S.; Formal analysis, C.N., P.W. and D.S.S.; Funding acquisition, D.S.S.; Investigation, S.W., C.N., P.J. and D.S.S.; Methodology, S.W., C.N., P.J. and D.S.S.; Project administration, D.S.S.; Resources, P.W., P.S., W.W. and D.S.S.; Supervision, D.S.S.; Validation, D.S.S.; Visualization, S.W., C.N., P.J. and D.S.S.; Writing—original

draft, S.W., C.N. and D.S.S.; Writing—review & editing, C.N. and D.S.S. All authors have read and agreed to the published version of the manuscript.

**Funding:** This research study was supported by the National Science, Research and Innovation Fund (NSRF) [Grant No. MET6601147S] and the Faculty of Medical Technology Research Fund, Prince of Songkla University.

**Institutional Review Board Statement:** Not applicable.

**Data Availability Statement:** The raw data are available from the corresponding author by request.

**Conflicts of Interest:** The authors declare no conflicts of interest.

## References

1. Yazarlu, O.; Iranshahi, M.; Kashani, H.R.K.; Reshadat, S.; Habtemariam, S.; Iranshahi, M.; Hasanpour, M. Perspective on the application of medicinal plants and natural products in wound healing: A mechanistic review. *Pharmacol. Res. Commun.* **2021**, *174*, 105841. [[CrossRef](#)] [[PubMed](#)]
2. Sen, C.K. Human wounds and its burden: An updated compendium of estimates. *Adv. Wound Care* **2019**, *8*, 39–48. [[CrossRef](#)] [[PubMed](#)]
3. Rodrigues, M.; Kosaric, N.; Bonham, C.A.; Gurtner, G.C. Wound healing: A cellular perspective. *Physiol. Rev.* **2019**, *99*, 665–706. [[CrossRef](#)] [[PubMed](#)]
4. Tao, G.; Cai, R.; Wang, Y.; Liu, L.; Zuo, H.; Zhao, P.; Umar, A.; Mao, C.; Xia, Q.; He, H. Bioinspired design of AgNPs embedded silk sericin-based sponges for efficiently combating bacteria and promoting wound healing. *Mater. Des.* **2019**, *180*, 107940. [[CrossRef](#)]
5. Munir, F.; Tahir, H.M.; Ali, S.; Ali, A.; Tehreem, A.; Zaidi, S.; Adnan, M.; Ijaz, F. Characterization and evaluation of silk sericin-based hydrogel: A promising biomaterial for efficient healing of acute wounds. *ACS Omega* **2023**, *8*, 32090–32098. [[CrossRef](#)]
6. Chouhan, D.; Mandal, B.B. Silk biomaterials in wound healing and skin regeneration therapeutics: From bench to bedside. *Acta Biomater.* **2020**, *103*, 24–51. [[CrossRef](#)]
7. Mondal, M.I.H.; Islam, M.M.; Haque, M.I.; Ahmed, F. Natural, biodegradable, biocompatible and bioresorbable medical textile materials. In *Medical Textiles from Natural Resources*; Elsevier: Amsterdam, The Netherlands, 2022; pp. 87–116.
8. Ruzsyzmah, B.H.I.; Chowdhury, S.R.; Manan, N.A.B.A.; Fong, O.S.; Adenan, M.I.; Saim, A.B. Aqueous extract of *Centella asiatica* promotes corneal epithelium wound healing in vitro. *J. Ethnopharmacol.* **2012**, *140*, 333–338. [[CrossRef](#)]
9. Radenahmad, N.; Saleh, F.; Sayoh, I.; Sawangiaroen, K.; Subhadhirasakul, P.; Boonyoung, P.; Rundorn, W.; Mitranun, W. Young coconut juice can accelerate the healing process of cutaneous wounds. *BMC Complement. Altern. Med.* **2012**, *12*, 252. [[CrossRef](#)]
10. Arango, M.C.; Montoya, Y.; Peresin, M.S.; Bustamante, J.; Álvarez-López, C. Silk sericin as a biomaterial for tissue engineering: A review. *Int. J. Polym. Mater.* **2021**, *70*, 1115–1129. [[CrossRef](#)]
11. Silva, A.S.; Costa, E.C.; Reis, S.; Spencer, C.; Calhelha, R.C.; Miguel, S.P.; Ribeiro, M.P.; Barros, L.; Vaz, J.A.; Coutinho, P. Silk Sericin: A promising sustainable biomaterial for biomedical and pharmaceutical applications. *Polymers* **2022**, *14*, 4931. [[CrossRef](#)]
12. Liu, J.; Shi, L.; Deng, Y.; Zou, M.; Cai, B.; Song, Y.; Wang, Z.; Wang, L. Silk sericin-based materials for biomedical applications. *Biomaterials* **2022**, *287*, 121638. [[CrossRef](#)] [[PubMed](#)]
13. Rahimpour, S.; Jabbari, H.; Yousofi, H.; Fathi, A.; Mahmoodi, S.; Jafarian, M.J.; Shomali, N.; Shotorbani, S.S. Regulatory effect of sericin protein in inflammatory pathways; A comprehensive review. *Pathol. Res. Pract.* **2023**, *243*, 154369. [[CrossRef](#)] [[PubMed](#)]
14. Manesa, K.C.; Kebede, T.G.; Dube, S.; Nindi, M.M. Fabrication and characterization of sericin-PVA composite films from *Gonometa postica*, *Gonometa rufobrunnea*, and *Argema mimosae*: Potentially applicable in biomaterials. *ACS Omega* **2022**, *7*, 19328–19336. [[CrossRef](#)]
15. Bakhsheshi-Rad, H.R.; Ismail, A.F.; Aziz, M.; Akbari, M.; Hadisi, Z.; Omid, M.; Chen, X. Development of the PVA/CS nanofibers containing silk protein sericin as a wound dressing: In vitro and in vivo assessment. *Int. J. Biol. Macromol.* **2020**, *149*, 513–521. [[CrossRef](#)]
16. Liu, B.; Zhang, J.; Guo, H. Research progress of polyvinyl alcohol water-resistant film materials. *Membranes* **2022**, *12*, 347. [[CrossRef](#)]
17. He, H.; Cai, R.; Wang, Y.; Tao, G.; Guo, P.; Zuo, H.; Chen, L.; Liu, X.; Zhao, P.; Xia, Q. Preparation and characterization of silk sericin/PVA blend film with silver nanoparticles for potential antimicrobial application. *Int. J. Biol. Macromol.* **2017**, *104*, 457–464. [[CrossRef](#)]
18. Khasraghi, A.H.; Thomas, L.M. Preparation and evaluation of lornoxicam film-forming gel. *Drug Inven. Today* **2019**, *11*, 1906–1913.
19. Noosak, C.; Jantorn, P.; Meesane, J.; Voravuthikunchai, S.; Saeloh, D. Dual-functional bioactive silk sericin for osteoblast responses and osteomyelitis treatment. *PLoS ONE* **2022**, *17*, e0264795. [[CrossRef](#)]
20. Pichayakorn, W.; Suksaeree, J.; Boonme, P.; Amnuaitik, T.; Taweeprada, W.; Ritthidej, G.C. Deproteinized natural rubber film forming polymeric solutions for nicotine transdermal delivery. *Pharm. Dev. Technol.* **2013**, *18*, 1111–1121. [[CrossRef](#)]

21. Sumayya, A.S.; Muraleedhara Kurup, G. In vitro anti-inflammatory potential of marine macromolecules cross-linked bio-composite scaffold on LPS stimulated RAW 264.7 macrophage cells for cartilage tissue engineering applications. *J. Biomater. Sci. Polym. Ed.* **2021**, *32*, 1040–1056. [\[CrossRef\]](#)
22. Pugar, D.; Haramina, T.; Leskovic, M.; Ćurković, L. Preparation and characterization of poly(vinyl-alcohol)/chitosan polymer blend films chemically crosslinked with glutaraldehyde: Mechanical and thermal investigations. *Molecules* **2024**, *29*, 5914. [\[CrossRef\]](#) [\[PubMed\]](#)
23. Jiang, K.; Li, J.; Brennan, M.; Brennan, C.; Chen, H.; Qin, Y.; Yuan, M. Smart indicator film based on sodium alginate/polyvinyl alcohol/TiO<sub>2</sub> containing purple garlic peel extract for visual monitoring of beef freshness. *Polymers* **2023**, *15*, 4308. [\[CrossRef\]](#) [\[PubMed\]](#)
24. Entekhabi, E.; Haghbin Nazarpak, M.; Sedighi, M.; Kazemzadeh, A. Predicting degradation rate of genipin cross-linked gelatin scaffolds with machine learning. *Mater. Sci. Eng. C* **2020**, *107*, 110362. [\[CrossRef\]](#) [\[PubMed\]](#)
25. Jin, S.G. Production and application of biomaterials based on polyvinyl alcohol (PVA) as wound dressing. *Chem. Asian J.* **2022**, *17*, e202200595. [\[CrossRef\]](#)
26. Noosak, C.; Iamthanaporn, K.; Meesane, J.; Voravuthikunchai, S.P.; Sotthibandhu, D.S. Bioactive functional sericin/polyvinyl alcohol hydrogel: Biomaterials for supporting orthopedic surgery in osteomyelitis. *J. Mater. Sci.* **2023**, *58*, 5477–5488. [\[CrossRef\]](#)
27. Dinescu, S.; Galateanu, B.; Albu, M.; Cimpean, A.; Dinischiotu, A.; Costache, M. Sericin enhances the bioperformance of collagen-based matrices preseeded with human-adipose derived stem cells (hADSCs). *Int. J. Mol. Sci.* **2013**, *14*, 1870–1889. [\[CrossRef\]](#)
28. Nursal, F.K.; Nining; Rahmani, A. Effect of glycerin as plasticizer in formulation of grape seed oil (*Vitis vinifera* L.) emulgel peel-off mask. In *IOP Conference Series: Earth and Environmental Science*; IOP Publishing Ltd.: Bristol, UK, 2021.
29. Wang, X.; Yucel, T.; Lu, Q.; Hu, X.; Kaplan, D.L. Silk nanospheres and microspheres from silk/PVA blend films for drug delivery. *Biomaterials* **2010**, *31*, 1025–1035. [\[CrossRef\]](#)
30. Parhi, R.; Goli, V.V.N. Design and optimization of film-forming gel of etoricoxib using research surface methodology. *Drug Deliv. Transl. Res.* **2020**, *10*, 498–514. [\[CrossRef\]](#)
31. Neha, V.; Saudagar, R. Formulation, development and evaluation of film-forming gel for prolonged dermal delivery of terbinafine hydrochloride. *Int. J. Pharma Sci. Res.* **2014**, *5*, 537–554.
32. Thanh, N.Q.; Mai, D.H.; Le, T.P.A.; Do, N.H.; Le, P.K. Novel chitosan/polyvinyl alcohol gel encapsulating ethanolic *Centella asiatica* extract for cosmeceutical applications. *Polym. Bull.* **2025**, *82*, 523–541. [\[CrossRef\]](#)
33. Monton, C.; Luprasong, C.; Suksaeree, J.; Songsak, T. Preparation and evaluation of film forming polymeric dispersion containing *Centella asiatica* extract for skin application. *Int. J. Pharma Sci. Res.* **2021**, *21*, 73–81. [\[CrossRef\]](#)
34. Lukić, M.; Pantelić, I.; Savić, S.D. Towards optimal pH of the skin and topical formulations: From the current state of the art to tailored products. *Cosmetics* **2021**, *8*, 69. [\[CrossRef\]](#)
35. Lambers, H.; Piessens, S.; Bloem, A.; Pronk, H.; Finkel, P. Natural skin surface pH is on average below 5, which is beneficial for its resident flora. *Int. J. Cosmet. Sci.* **2006**, *28*, 359–370. [\[CrossRef\]](#)
36. Aramwit, P.; Siritientong, T.; Srichana, T. Potential applications of silk sericin, a natural protein from textile industry by-products. *Waste Manag. Res.* **2011**, *30*, 217–224. [\[CrossRef\]](#)
37. Djiobie Tchienou, G.E.; Tsatsop Tsague, R.K.; Mbam Pega, T.F.; Bama, V.; Bamseck, A.; Dongmo Sokeng, S.; Ngassoum, M.B. Multi-response optimization in the formulation of a topical cream from natural ingredients. *Cosmetics* **2018**, *5*, 7. [\[CrossRef\]](#)
38. Elkhenany, H.; Abou-Shanab, A.M.; Magdy, S.; Kamar, S.S.; Salah, R.A.; El Badri, N. Comprehensive evaluation of ethanol-preserved amniotic extracts: Exploring antioxidant properties, proliferation enhancement, protective efficacy and regeneration potential in wound healing. *J. Drug Deliv. Sci. Technol.* **2024**, *100*, 106062. [\[CrossRef\]](#)
39. Marto, J.; Baltazar, D.; Duarte, A.; Fernandes, A.; Gouveia, L.; Militão, M.; Salgado, A.; Simões, S.; Oliveira, E.; Ribeiro, H.M. Topical gels of etofenamate: In vitro and in vivo evaluation. *Pharm. Dev. Technol.* **2015**, *20*, 710–715. [\[CrossRef\]](#)
40. Gennari, C.G.M.; Selmin, F.; Ortenzi, M.A.; Franzé, S.; Musazzi, U.M.; Casiraghi, A.; Minghetti, P.; Cilurzo, F. In situ film forming fibroin gel intended for cutaneous administration. *Int. J. Pharm.* **2016**, *511*, 296–302. [\[CrossRef\]](#)
41. Dubey, V.; Daschakraborty, S. Influence of glycerol on the cooling effect of pair hydrophobicity in water: Relevance to proteins' stabilization at low temperature. *Phys. Chem. Chem. Phys.* **2019**, *21*, 800–812. [\[CrossRef\]](#)
42. Kang, S.-Y.; Um, J.-Y.; Chung, B.-Y.; Lee, S.-Y.; Park, J.-S.; Kim, J.-C.; Park, C.-W.; Kim, H.-O. Moisturizer in patients with inflammatory skin diseases. *Medicina* **2022**, *58*, 888. [\[CrossRef\]](#)
43. Manesa, K.C.; Kebede, T.G.; Dube, S.; Nindi, M.M. Profiling of silk sericin from cocoons of Three Southern African wild silk moths with a focus on their antimicrobial and antioxidant properties. *Materials* **2020**, *13*, 5706. [\[CrossRef\]](#) [\[PubMed\]](#)
44. Kunz, R.; Brancalhão, R.M.C.; Ribeiro, L.; Natali, M. Silkworm sericin: Properties and biomedical applications. *Biomed. Res. Int.* **2016**, *2016*, 8175701. [\[CrossRef\]](#) [\[PubMed\]](#)

45. Baptista-Silva, S.; Borges, S.; Costa-Pinto, A.R.; Costa, R.; Amorim, M.; Dias, J.R.; Ramos, Ó.; Alves, P.; Granja, P.L.; Soares, R.; et al. In situ forming silk sericin-based hydrogel: A novel wound healing biomaterial. *ACS Biomater. Sci. Eng.* **2021**, *7*, 1573–1586. [[CrossRef](#)] [[PubMed](#)]
46. Jeong, H.-L.; Kang, E.-B.; Yun, S.-G.; Park, D.-b.; Lim, J.-O.; Suh, J.-S. Effect of a silk sericin and Methylsulfonylmethane (MSM) blends on inflammatory response and wound healing. *Appl. Sci.* **2023**, *13*, 288. [[CrossRef](#)]
47. Prakash, M.; Mathikere Naganna, C.; Radhakrishnan, V.; Somayaji, P.; Sabu, L. Therapeutic potential of silkworm sericin in wound healing applications. *Wound Repair Regen.* **2024**, *32*, 916–940. [[CrossRef](#)]
48. Cam, M.; Yildiz, S.; Alenezi, H.; Cesur, S.; Ozcan, G.; Erdemir Cilasun, G.; Edirisinghe, U.; Akakin, D.; Kuruca, D.; Kabasakal, L.; et al. Evaluation of burst release and sustained release of pioglitazone-loaded fibrous mats on diabetic wound healing: An in vitro and in vivo comparison study. *J. R. Soc. Interface.* **2020**, *17*, 20190712. [[CrossRef](#)]
49. Andrabi, S.M.; Sharma, N.S.; Karan, A.; Shahriar, S.M.S.; Cordon, B.; Ma, B.; Xie, J. Nitric oxide: Physiological functions, delivery, and biomedical applications. *Adv. Sci.* **2023**, *10*, e2303259. [[CrossRef](#)]
50. Cai, X.; Sha, F.; Zhao, C.; Zheng, Z.; Zhao, S.; Zhu, Z.; Zhu, H.; Chen, J.; Chen, Y. Synthesis and anti-inflammatory activity of novel steroidal chalcones with 3 $\beta$ -pregnenolone ester derivatives in RAW 264.7 cells in vitro. *Steroids* **2021**, *171*, 108830. [[CrossRef](#)]
51. Xie, C.; Li, X.; Zhu, J.; Wu, J.; Geng, S.; Zhong, C. Magnesium isoglycyrrhizinate suppresses LPS-induced inflammation and oxidative stress through inhibiting NF- $\kappa$ B and MAPK pathways in RAW264.7 cells. *Bioorg. Med. Chem.* **2019**, *27*, 516–524.
52. Mu, K.; Yu, S.; Kitts, D.D. The role of Nitric Oxide in regulating intestinal redox status and intestinal epithelial cell functionality. *Int. J. Mol. Sci.* **2019**, *20*, 1755. [[CrossRef](#)]
53. Anavi, S.; Tirosh, O. iNOS as a metabolic enzyme under stress conditions. *Free Radic. Biol. Med.* **2020**, *146*, 16–35. [[CrossRef](#)] [[PubMed](#)]
54. Mukherjee, S.; Dutta, S.; Pati, S.; Sarkar, T.; Paul, S.; Chakraborty, S.; Basak, U.; Dhar, S.; Das, T.; Sa, G. Nuclear factor kappa-B: The El Dorado of inflammatory immune response. *Cell. Mol. Immunol.* **2024**, *3*, 6–19. [[CrossRef](#)]
55. Surh, Y.J.; Chun, K.S.; Cha, H.H.; Han, S.S.; Keum, Y.S.; Park, K.K.; Lee, S.S. Molecular mechanisms underlying chemopreventive activities of anti-inflammatory phytochemicals: Down-regulation of COX-2 and iNOS through suppression of NF-kappa B activation. *Mutat. Res.* **2001**, *480–481*, 243–268. [[CrossRef](#)] [[PubMed](#)]
56. Aramwit, P.; Towiwat, P.; Srichana, T. Anti-inflammatory potential of silk sericin. *Nat. Prod. Commun.* **2013**, *8*, 501–504. [[CrossRef](#)]
57. Sun, Y.; Shi, W.; Zhang, Q.; Guo, H.; Dong, Z.; Zhao, P.; Xia, Q. Multi-omics integration to reveal the mechanism of sericin inhibiting LPS-induced inflammation. *Int. J. Mol. Sci.* **2022**, *24*, 259. [[CrossRef](#)]

**Disclaimer/Publisher’s Note:** The statements, opinions and data contained in all publications are solely those of the individual author(s) and contributor(s) and not of MDPI and/or the editor(s). MDPI and/or the editor(s) disclaim responsibility for any injury to people or property resulting from any ideas, methods, instructions or products referred to in the content.